

Formation of lipid bilayer membrane in a poly(dimethylsiloxane) microchip integrated with a stacked polycarbonate membrane support and an on-site nanoinjector

Wei Teng, Changill Ban, and Jong Hoon Hahn

Citation: *Biomicrofluidics* **9**, 024120 (2015); doi: 10.1063/1.4919066

View online: <http://dx.doi.org/10.1063/1.4919066>

View Table of Contents: <http://scitation.aip.org/content/aip/journal/bmf/9/2?ver=pdfcov>

Published by the [AIP Publishing](#)

Articles you may be interested in

[Screening ion-channel ligand interactions with passive pumping in a microfluidic bilayer lipid membrane chip](#)
Biomicrofluidics **9**, 014103 (2015); 10.1063/1.4905313

[Physical understanding of pore formation on supported lipid bilayer by bacterial toxins](#)
AIP Conf. Proc. **1512**, 156 (2013); 10.1063/1.4790958

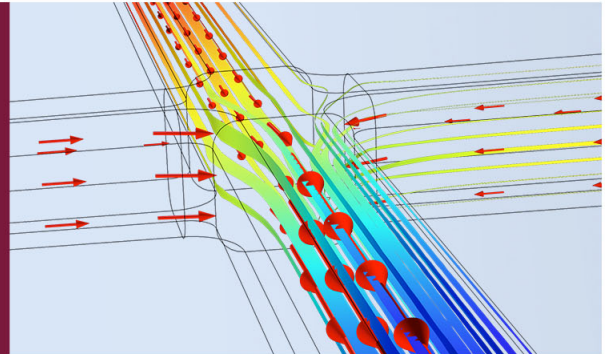

[Effect of integral proteins in the phase stability of a lipid bilayer: Application to raft formation in cell membranes](#)
J. Chem. Phys. **132**, 135104 (2010); 10.1063/1.3381179

[Discrete and heterogeneous rotational dynamics of single membrane probe dyes in gel phase supported lipid bilayer](#)
J. Chem. Phys. **120**, 3030 (2004); 10.1063/1.1640349

[Effect of strong magnetic fields on the characteristics of bilayer lipid membranes](#)
J. Appl. Phys. **81**, 4318 (1997); 10.1063/1.364755

How to Simulate & Design Microfluidics Devices

COMSOL



Formation of lipid bilayer membrane in a poly(dimethylsiloxane) microchip integrated with a stacked polycarbonate membrane support and an on-site nanoinjector

Wei Teng, Changill Ban, and Jong Hoon Hahn^{a)}

Department of Chemistry, BioNanotechnology Center, Pohang University of Science and Technology, 77 Cheongam-Ro, Nam-Gu, 790-784 Pohang, South Korea

(Received 11 February 2015; accepted 14 April 2015; published online 22 April 2015)

This paper describes a new and facile approach for the formation of pore-spanning bilayer lipid membranes (BLMs) within a poly(dimethylsiloxane) (PDMS) microfluidic device. Commercially, readily available polycarbonate (PC) membranes are employed for the support of BLMs. PC sheets with 5 μm , 2 μm , and 0.4 μm pore diameters, respectively, are thermally bonded into a multilayer-stack, reducing the pore density of 0.4 μm -pore PC by a factor of 200. The BLMs on this support are considerably stable (a mean lifetime: 17 h). This multilayer-stack PC (MSPC) membrane is integrated into the PDMS chip by an epoxy bonding method developed to secure durable bonding under the use of organic solvents. The microchip has a special channel for guiding a micropipette in the proximity of the MSPC support. With this on-site injection technique, tens to hundreds of nanoliters of solutions can be directly dispensed to the support. Incorporating gramicidin ion channels into BLMs on the MSPC support has confirmed the formation of single BLMs, which is based on the observation from current signals of 20 pS conductance that is typical to single channel opening. Based on the bilayer capacitance (1.4 pF), about 15% of through pores across the MSPC membrane are estimated to be covered with BLMs. © 2015 AIP Publishing LLC.

[<http://dx.doi.org/10.1063/1.4919066>]

I. INTRODUCTION

Cellular membranes form a barrier to enclose cytoplasm and organelles within the cell, but they are not merely passive barriers. Membranes include a wide range of proteins specialized for various physiological and biochemical processes: passive and active transport of materials, recognition of external substances, intercellular communication, signal transduction, etc. Understanding how membrane proteins function in cellular systems has received a great deal of interests over decades.¹ Membrane proteins are the targets of one third of pharmaceutical drugs.² Among many different membrane proteins, ion channels are well recognized as a major class of drug targets. The current process for drug discovery, however, has been becoming more complex. For example, in developing an ion channel-targeted drug, it requires screening of an extremely large number of compounds against the ion channel target, and then the drug candidates selected from the library screening should be tested through ion channel screening if they can significantly disrupt the normal physiology.

For over four decades, patch clamping³ and planar bilayer methods⁴ have been extensively used in investigating the properties of ion channels. The planar bilayer method offers some advantages over patch clamping: for examples, no interference from other membrane proteins and easy control of experimental parameters (buffer pH, lipid composition, etc.). The method

^{a)} Author to whom correspondence should be addressed. Electronic mail: hahn@postech.edu

has also provided stable bilayer lipid membranes (BLMs) by thinning the septum^{5,6} or narrowing the aperture to sub-microscale (0.1–1 μm)^{7–9} and nanoscale (1–100 nm).¹⁰ However, making such apertures demands sophisticated equipment, cumbersome fabrication procedure, high manufacturing cost, etc.

Microfluidics has been extensively employed for formation of lipid vesicles.^{11,12} Recently, approaches to prepare the planar lipid bilayers in microfluidic systems have been proposed,^{13–15} because the microfluidic platform has advantages for facilitating BLM study: for example, it provides minimal volumes for the electrolyte solution chambers on both sides of membrane, and endows the potential to be evolved for automated, high-throughput drug screening. The applicability of such microfluidic BLM platforms has been demonstrated mainly through the reconstitution of functional ion channels by the self-insertion method.^{16–18} Zagnoni *et al.* have extended the applicability to large membrane proteins by developing the proteoliposome fusion method.¹⁹ Some of these microfluidic BLM platforms use open-well types where solutions are applied via a micropipette to apertures or membranes from the open side.^{17,19} Since the solutions are subjected to evaporation and contamination, such systems are not suitable for prolonged analyses. Some platforms use enclosed microfluidic devices where BLMs are formed on the zone between the top and bottom microchannels.^{16,18}

This paper reports the development of a microchip-based BLM system coupled with the technique of direct solution injection on the membrane site. Stable BLMs are formed on a multilayer-stack polycarbonate (MSPC) membrane with micro- or submicro-pores. The membrane is fabricated by plasma-enhanced thermal bonding of multiple, commercially available polycarbonate (PC) membranes, which offer a facile and low-cost alternative to the common, microfabrication-based preparation of submicropores.⁸ The MSPC membrane is then integrated into the poly(dimethylsiloxane) (PDMS) microchip by an epoxy bonding technique that we have developed to provide strong bonding between PDMS and MSPC even under organic solvents. By taking advantage of the elasticity of PDMS, an injection micropipette can be positioned on the site of the MSPC membrane standing on the zone crossed by the top and bottom microchannels of our enclosed microfluidic system. This on-site injection technique facilitates solution exchange, BLM formation, ion channel incorporation, etc.

II. MATERIALS AND METHODS

A. Microfabrication of device

1. Microchannel design

Our PDMS microfluidic device has dimensions of 40 mm \times 30 mm \times 3 mm. As illustrated in Fig. 1(a), it consists of three parts: (1) the upper PDMS plate having, on its bottom surface, a top microchannel groove and a dead-end micropipette-guiding channel groove, (2) an MSPC membrane with micro- or sub-micropores, and (3) the lower PDMS plate with a bottom microchannel groove on its top surface. The top and bottom microchannels (400 μm in width and 200 μm in depth) are aligned to be perpendicular to each other (Figs. 1(b) and 1(c)) in a way that an MSPC membrane over which BLMs are formed is actually free standing at the cross zone intersected by the two microchannels. The number of pores in the zone is, therefore, simply controlled by the widths of the two microchannels. The microchannel for guiding an injection micropipette is used to locate the tip of the micropipette at the correct position (close to the cross zone in the top channel) after the sharp tip punctures the thin PDMS wall (thickness: ca. 350 μm , Fig. S1 in the supplementary material²⁰) between the guiding channel end and the top channel.

2. MSPC membrane fabrication

Both surfaces of PC membranes (Hydrophobic polycarbonate track-etched membranes, Sterlitech, Kent, WA, USA) are treated in an O₂ plasma chamber (PDC-32G, Harrick Plasma, Ithaca, NY, USA) for 90 s at a radio-frequency power of 18W. A multilayer stack of the activated PC membranes is then sandwiched in between two quartz plates of good flatness. The

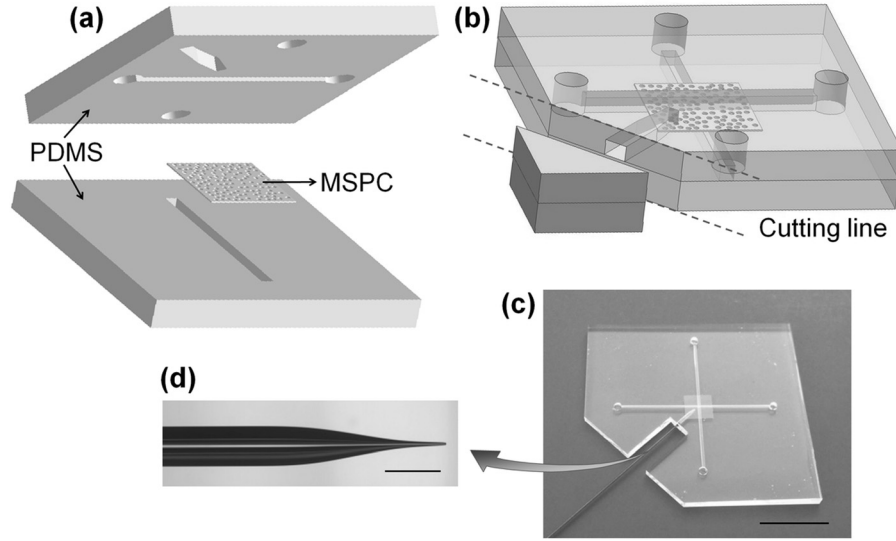


FIG. 1. Schematic diagram of an MSPC-integrated microfluidic system for BLM formation. (a) and (b) Conceptual graphs of a microfluidic device including the top and bottom microchannels crossed at a right angle, a dead-end guiding channel designed to aid micropipette insertion into the top microchannel, and a porous MSPC membrane as BLM support. An access to the guiding channel is made by cutting off a part of the microdevice. (c) Photograph of a typical microdevice with a micropipette inserted via the on-site injection method (Fig. S3 in the supplementary material²⁰). (d) Optical micrograph of the micropipette shown in (c). Scale bars, 1 cm (c), 500 μm (d). (For the dimensions of microchannels, see Fig. S1 in the supplementary material.²⁰)

assembly is clamped (Fig. S2 in the supplementary material²⁰), and degassed under vacuum for 10 min. Thermal bonding between PC membranes in the stack is accomplished by placing the clamped assembly in a convection oven at 165 °C for 25 min. The appearance of MSPC membrane is translucent. Occasionally, overheating or unbalanced clamping generates transparent spots on it.

3. MSPC membrane integration

EPO-TEK[®] 377 (Epoxy Technology, Billerica, MA, USA) has been chosen for bonding the MSPC membrane with two PDMS plates, because the company claims that the epoxy is the most moisture- and chemical-resistant adhesive in their line of medical adhesives.²¹ The two parts of the product are mixed at 1:1 ratio by weight, and a small amount of xylene is added into the mixture (epoxy:xylene = 20:1 by weight) to improve the wettability of the epoxy on glass and PDMS. The resin solution is then spun on a Piranha-cleaned glass slide (Corning Inc., Corning, NY, USA) at 3500 rpm for 60 s to generate a thin glue layer with a thickness of ca. 50 μm . Immediately after the top surface of the lower PDMS plate is treated with O₂ plasma, the surface is stamped onto the epoxy-coated glass slide for 5 min, and then the plate is peeled off from it. A 5 mm \times 5 mm piece of the MSPC membrane is placed across the microchannel groove on the glue-coated PDMS surface. This MSPC-attached plate is aligned and evenly contacted with the epoxy-coated upper plate, so that it leaves a standing MSPC-membrane region at the zone crossed by the top and bottom microchannels. The fabrication of an MSPC-membrane-integrated PDMS microchip is completed by placing the assembly in a 120 °C oven for 2 h for curing epoxy.

B. Bonding strength analysis: Leakage and peel tests

In two ways, leakage and peel tests, we have examined the bonding between PDMS plates and the MSPC membrane. In the leakage test, fluorescein solution (13 μM fluorescein sodium salt (F6377, Sigma-Aldrich, St. Louis, MO, USA) in 1 M KCl, 10 mM PBS solution (pH 7.4, abbreviated as KCl buffer)) is flowed into the top and bottom microchannels at a flow rate of

$10 \mu\text{l min}^{-1}$ for 30 min. The fluorescence imaging has been conducted on a CCD-equipped inverted microscope (Eclipse TE2000-U, Nikon Corporation, Tokyo, Japan) to check for leakages. In the peel test, decane is pumped into the top and bottom microchannels at a flow rate of $10 \mu\text{l min}^{-1}$ for 30 min, and then drained out. An access to the cross section of PDMS-MSPC assembly is made by cutting off a part of microchip (see cutting line A-A' in Fig. 2(a)). A pair of tweezers is used as a two-pronged hook to pull the assembly apart (Fig. 2(c)). Two other bonding methods have been also evaluated on the same tests. In one method, an MSPC membrane is integrated into the PDMS microchip using PDMS prepolymer as glue.²² In the other, 3-aminopropyltriethoxysilane (APTES) is used as a chemical agent to crosslink PDMS with PC.²³

C. Preparation of on-site injection micropipettes

Fused-silica capillary (O.D. = $360 \mu\text{m}$, I.D. = $100 \mu\text{m}$; Polymicro Technology, Phoenix, AZ, USA) is used to prepare injection micropipettes.^{24,25} Fused-silica capillaries are pulled with a microprocessor-controlled CO_2 laser-based puller (P-2000, Sutter Instruments, Novato, CA, USA). A pulling program (Table SI in the supplementary material²⁰) has been developed to produce a short “needle” (patch type) with the tip diameter of $\sim 0.5 \mu\text{m}$ and the taper length of $\sim 1.5 \text{mm}$. The tip of a pulled capillary is then beveled at an angle of 20° with a micropipette beveller (BV-10, Sutter Instruments, Novato, CA, USA) for easy penetration into the PDMS side wall. The injection micropipette is connected to a gas-tight syringe ($500 \mu\text{l}$, Hamilton, Reno, NV, USA), and mounted onto a three-axis hydraulic manipulator (MHW-3, Narishige Group, East Meadow, NY, USA) to control ultrafine three-dimensional movement with an accuracy of 200nm (Figs. S3(d) and S3(e) in the supplementary material²⁰). Solution injection of the desired volume in the range of tens to hundreds of nanoliters can be easily controlled by plunger displacement.

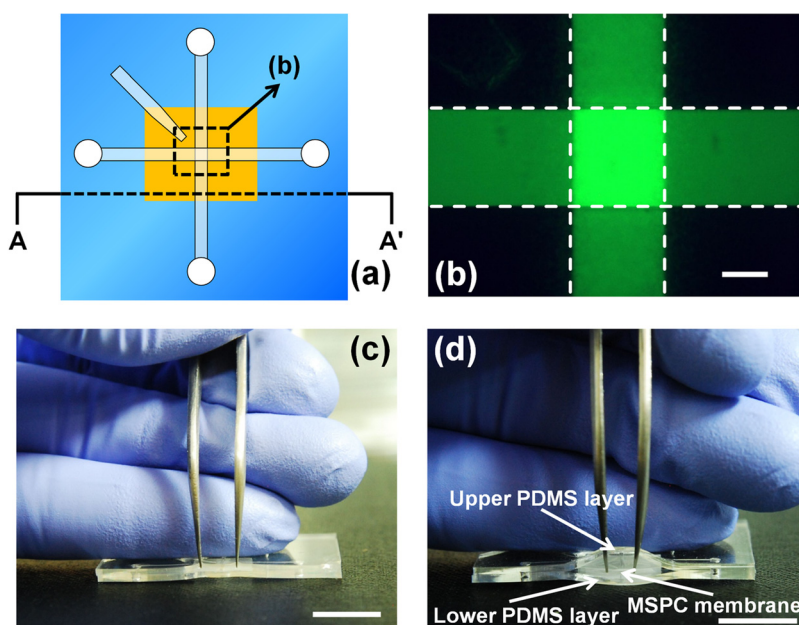


FIG. 2. Bonding strength tests. (a) A drawing of chip layout. The yellow rectangle denotes the integrated MSPC membrane. (b) Optical micrograph of fluorescein-filled microchannels (fabricated by an epoxy bonding technique), corresponding to the dashed rectangle in (a). The white dashed lines indicate microchannels. (c) Peel test of MSPC-integrated PDMS microchip bonded by epoxy bonding technique. The cross sections shown in (c) and (d) are accessed by cutting the chip along the dashed line A-A' in (a). (c) shows PDMS layers, and the MSPC membrane could not be peeled from each other. (d) shows the result of the unsuccessful bonding. PDMS layers are separated from the MSPC membrane. Scale bars, $200 \mu\text{m}$ (b), 1cm (c) and (d). (For the other results of bonding strength tests, see Figs. S4 and S5 in the supplementary material.²⁰)

D. Preparation of DPhPC lipid solution

DPhPC (1,2-diphytanoyl-*sn*-glycero-3-phosphocholine) is dissolved in chloroform. The solvent of the DPhPC solution is evaporated under a stream of nitrogen at room temperature to form a thin lipid film on the bottom of a glass vial. The vial is connected to a vacuum line (<500 mTorr) for at least 2 h to remove the residual solvent. The dry lipid is then resolubilized with *n*-decane. DPhPC concentration of this stock solution is 20 mg ml^{-1} . The lipid solution is stored at -20°C before use.

E. BLM formation and ion channel incorporation

The lipid solution (20 mg ml^{-1} of DPhPC in decane) or the ion channel solution (1 ng ml^{-1} of gramicidin in ethanol) is directly injected over the integrated MSPC membrane with an injection micropipette. For this on-site injection, the micropipette is smoothly inserted into the guiding channel. With the aid of a microscope, the micropipette tip is placed within the top microchannel near the cross zone after puncturing the thin PDMS wall. To form BLMs on the MSPC membrane, first, intact surfaces of the submicropores formed in the membrane are primed by dispensing about 100 nl of the DPhPC solution over the membrane with the micropipette. As the organic solvent of the lipid solution is readily absorbed into the bulk of PDMS,^{26,27} the solution plug becomes smaller. When the solvent is fully absorbed, the top and bottom channels are filled with KCl buffer (Fig. 3(a)). About 75 nl of lipid solution is then dispensed (Fig. 3(b)). The volume of the lipid solution phase decreases as decane is absorbed by PDMS (Fig. 3(c)). When the solvent is completely absorbed, BLMs are formed over the membrane pores (Fig. 3(d)). In incorporating the ion channels into BLMs, about 25 nl of the gramicidin solution is injected over the BLM-formed MSPC membrane with an another micropipette. If the sealing resistance falls below $\text{G}\Omega$ level or no ion channel current is detected, rinsing and injection are repeated until bilayers are formed. The success rate of bilayer formation turns out

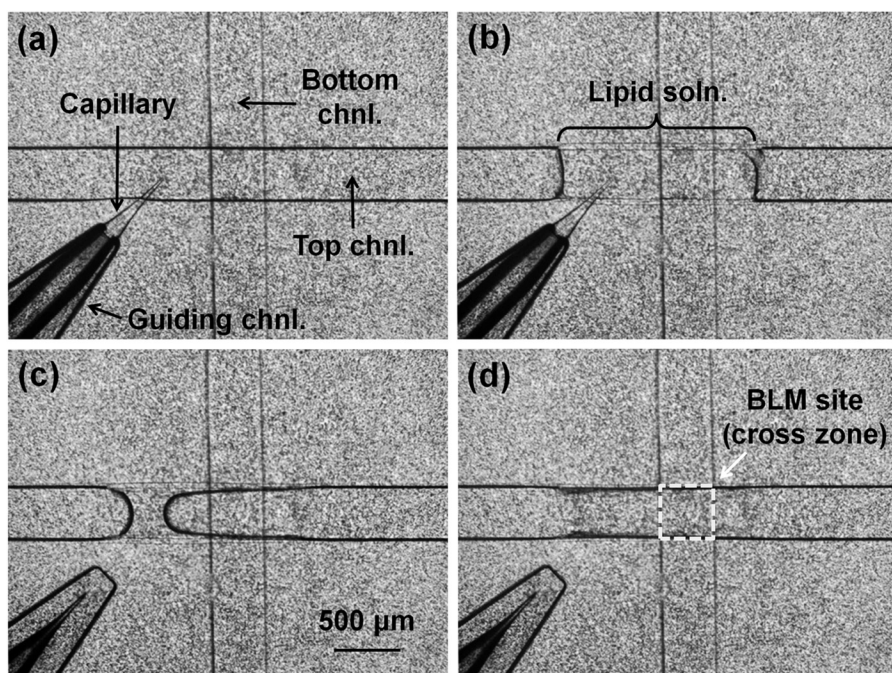


FIG. 3. Series of optical micrographs showing the process of BLM formation assisted by on-site injection technique. (a) Both top and bottom channels are filled with KCl buffer. Along the guiding channel, a micropipette is inserted into the top channel via a micromanipulator (see Fig. S3 in supplementary material²⁰ for details). (b) About 75 nl of lipid solution is injected into the top microchannel. (c) The volume of lipid solution phase becomes smaller as decane is gradually absorbed by PDMS. (d) After several minutes, the solvent is completely absorbed. BLM is formed over the pores of the MSPC membrane within the cross zone. Scale bar in panel (c) applies to all panels.

to be about 15%. After experiments, the chips are cleaned by flushing the microchannels with methanol and deionised water, and then placed in a convection oven at 70 °C overnight to ensure complete drying. Normally, the chip after such process can be reused at least 5 times with no significant change in BLM formation and stability.

F. Electrical measurements

The whole system for measuring current across the BLMs formed on an MSPC membrane is enclosed in a Faraday cage. BLM formation and ion channel incorporation are monitored electrically using two commercial Ag/AgCl electrodes placed in the reservoirs at the end of top and bottom microchannels, respectively. A function generator (33250 A, Agilent, Loveland, CO, USA) supplies a voltage profile between the two Ag/AgCl electrodes. The current thus generated by the applied voltage profile is converted into a voltage signal through a current amplifier (428-PROG, Keithley, Cleveland, OH, USA). The bandwidth of the amplifier is 3.5 kHz at the gain of 10^{10} V/A. The signal after amplification is filtered (the rise time: 3 ms) with a low-pass filter in the amplifier. The output voltage of the amplifier is monitored with an analog/digital storage oscilloscope (LT342, LeCroy, Chestnut Ridge, NY, USA), digitized via a multimeter (2010, Keithley, Cleveland, OH, USA), and stored on a PC using a LabView program (National Instruments, Austin, TX, USA). Bilayer capacitance is determined by applying a triangular wave²⁸ (50 mV amplitude and 5 Hz frequency), using a potentiostat (FAS2/Femtostat, Gamry Instruments, Warminster, PA, USA) set at an acquisition frequency of 2 kHz.

G. Cryostat sectioning

An MSPC membrane is embedded in the O.C.T. compound (Cat. No. 4583, Sakura/Tissue-Tek, Torrance, CA, USA), and stored at -80°C . Frozen sections ($6\ \mu\text{m}$ in thickness) are cut on a cryostat microtome (Leica CM 1800, Leica Instruments GmbH, Mannheim, Germany) at -25°C , and mounted onto glass slides for the subsequent microscopic observation (Fig. 4(c)).

An expended materials and methods section is provided in the supplementary material.²⁰

III. RESULTS AND DISCUSSION

A. Submicropore fabrication from commercial PC membranes

Currently, there is an increasing interest in the BLM formation over micropore filter membranes, because the conventional micro- or submicro-pore fabrication approaches demand complex instrumentation, cumbersome fabrication procedure, and high manufacturing cost.^{29,30} Among commercially available filter membranes, PC membrane has become one of the most suitable porous supports for the pore-spanning BLM formation,^{31–35} owing to its favorable characteristics, such as circular apertures of the greater regularity, smooth surfaces, and high resistivity. But, because of its high pore population, PC-supported BLMs are very susceptible to hydrodynamic pressure. For this reason, such BLMs have not been formed in a microfluidic system where hydraulic fluidics is involved. To address this issue, we propose the MSPC membrane (Fig. 4) to form the pore-spanning BLMs in a microfluidic system. The MSPC membrane is made up by thermal fusion bonding of several sheets of PC membranes of different pore sizes. To our knowledge, the bonding of such ultrathin thermoplastic layers ($\sim 10\ \mu\text{m}$) has not been reported before.

PC membranes are abundant with pores of submicro- and nanometer range (For example, the PC membrane of 400-nm pore diameter has the pore density of 1.5×10^8 pores cm^{-2}). Even a single pore that is not properly sealed by lipids, however, would be potentially fatal to ion channel current measurement. In this work, we propose a strategy to reduce the pore density. Multiple PC membranes are stacked in descending order of pore size. Since a PC membrane with bigger pores has lower pore density (Fig. 4(b) and Table SII in the supplementary material²⁰), the stacking efficiently blocks most of pores in the bottom-most layer, the pore size of which defines the aperture size of an MSPC membrane. The cross-sectional views of an MSPC membrane are taken with a field-emission scanning electron microscope (FESEM; JSM-

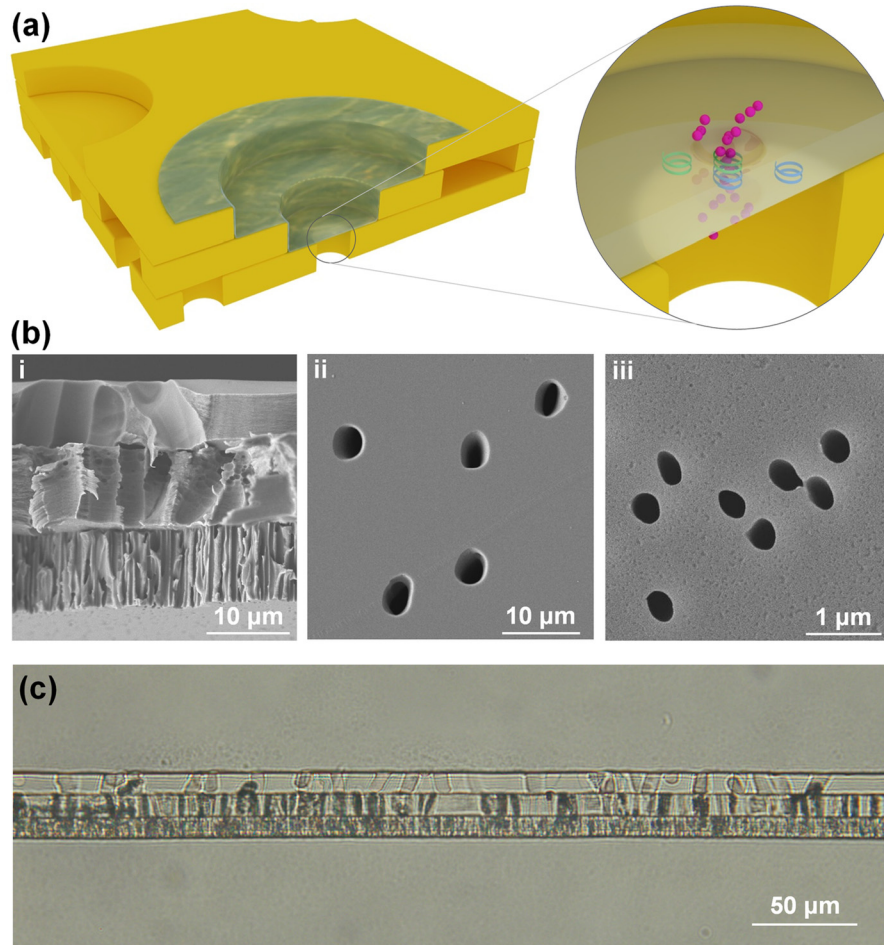


FIG. 4. Images of submicropore MSPC membrane. (a) Conceptual graph of a BLM-formed submicropore (not to scale). Cross section of a typical BLM site is shown. An MSPC membrane and a supported BLM are indicated by yellow and gray color, respectively. A close-up view shows that two gramicidin monomers (green and blue color) align to form an ion channel that allows the passage of monovalent cations (purple color). (b) FESEM images: (i) cross section view, (ii) top view, and (iii) bottom view of a three-layer MSPC membrane. (c) Optical micrograph of a microtome-processed three-layer MSPC membrane. The pore sizes from top to bottom layer for the MSPC membranes shown in (b) and (c) are $5\ \mu\text{m}$, $2\ \mu\text{m}$, and $0.4\ \mu\text{m}$.

7401F, JEOL, Tokyo, Japan) and an upright microscope (BX51, Olympus, Tokyo, Japan), which demonstrates that most of pores of the bottom-most layer are blocked by stacking of PC membranes (Figs. 4(b) and 4(c)). The MSPC membrane in Fig. 3 has 400-nm apertures to its bottom surface (panel (iii) in Fig. 4(b)). The lipid or ion channel solution is applied to its top surface ($5\text{-}\mu\text{m}$ pore side) with an injection micropipette.

B. On-site injection technique

Fig. 1 shows that the microchip designed to form BLMs has a special structural component: a guiding channel for an injection micropipette. Through this channel, the pipette is introduced into the chip, and the tip of the pipette, via puncturing the thin PDMS wall, can be accurately positioned at the predetermined location in a microfluidic channel. Thanks to the elasticity and hydrophobicity of PDMS—micropipette insertion into and withdrawal out of the microfluidic channel are not associated with solution leaking out and air rushing in. What is more, the $350\text{-}\mu\text{m}$ -thickness PDMS wall withstands micropipette insertion for at least 20 times. This on-site injection technique can reduce the amount of sample by 10^3 fold (from μl to nI), compared with the sample introduction in conventional microchips where solutions

are delivered to the site for BLM formation through the ends of microchannels. Of particular importance is it when precious samples and reagents should be used (e.g., expressed proteins). Therefore, by using our technique, only minimal amounts of different solutions can be sequentially dispensed directly on the site of BLM formation. Moreover, when a microfluidic system with multiple stations for different kinds of BLM is to be developed, our on-site injection technique would be especially advantageous because it could simplify the design of a microchannel network.

C. Integration of an MSPC membrane into a PDMS microchip

Gluing with PDMS prepolymer²² and conjugation by APTES²³ have been proposed for integrating a PC membrane into a PDMS microchip. Both methods have been applied to microchips only for the use of aqueous flows. In this work, however, we use decane as the solvent of the lipid solution. We have observed that the resistance across the MSPC membrane in the microchips fabricated by the two reported bonding techniques remains almost the same (tens to hundreds of k Ω) when we change the solution above the membrane from KCl buffer to the lipid solution that has a high resistance for electrical current. We have thought that decane breaks up the bonding between PDMS plates and the MSPC membrane, which causes electrical shortage between the top and bottom microchannels. To examine the bonding strength of these two methods, the microchips fabricated by them are subject to leakage and peel tests. To check for leakages, fluorescein solution is introduced into the top and bottom microchannels. In the peel test, the decane-treated microchips are pulled under the force vertical to the bonding interfaces. The microchips obtained from the PDMS prepolymer method fail in both tests (Figs. S4(a) and S5(b) in the supplementary material²⁰), whereas those from the APTES method show no leakage (Fig. S4(b) in the supplementary material²⁰) but fail in the peel test (Fig. 2(d)). To improve the strength in bonding under the use of organic solvents, we have developed a way of using epoxy adhesive, where we have chosen an epoxy product that is highly resistant to chemicals and doped xylene into the epoxy mixture. Xylene helps epoxy to be homogeneously transferred from the spin-coated glass slide to the plasma-treated PDMS plate. No leakages have been observed (Fig. 2(b)), and layers in the PDMS-MSPC assembly are not split by the force employed in the peel test (Fig. 2(c) and Fig. S5(a) in the supplementary material²⁰). The resistance value across the MSPC membrane increases in changing from KCl buffer to the lipid solution. Now the bonding is durable enough: it is reliable for repetitive BLM formations until a microchip should be discarded when the solution inside the top microchannel leaks out through the thin PDMS wall during the on-site injection.

D. Characterizations of pore-spanning BLMs

MSPC membranes with difference in layer stacking and pore diameters (0.4, 1, 2, and 5 μm ; specifications in Table SII of the supplementary material²⁰) have been tested to find the combinations with appreciable BLM stability. The BLM stability has been evaluated in terms of time during which the resistance remains higher than 1 G Ω , the sealing threshold.³⁶ BLMs on single PC membranes showed poor stability, regardless of the pore diameter, and the same went for 2-layer MSPCs. No matter how to make combinations of two component PC sheets with the same or different pore diameters, the resistance dropped from G Ω to M Ω shortly after the injection of lipid solution (1PC and 2PC in Fig. 5(a)). In 3-layer MSPCs, we have found that the pore diameter of the bottom-most PC layer is an important factor for attaining BLM stability. For instance, 3PCb membranes (5 μm |2 μm |0.4 μm) with 400-nm apertures have 13 times longer lifetime than 3PCa's (5 μm |2 μm |1 μm) with 1- μm apertures (Fig. 5(a)). In the case of 4-layer MSPC membranes, we have found from the electrical measurements of lipid-free membranes that through pores are hardly formed. Hence, we have used the 5 μm |2 μm |0.4 μm membrane for the rest of the study. A typical current–voltage relationship for BLMs on the MSPC membrane shows a seal resistance of 4.8 G Ω (Fig. S6 in the supplementary material²⁰).

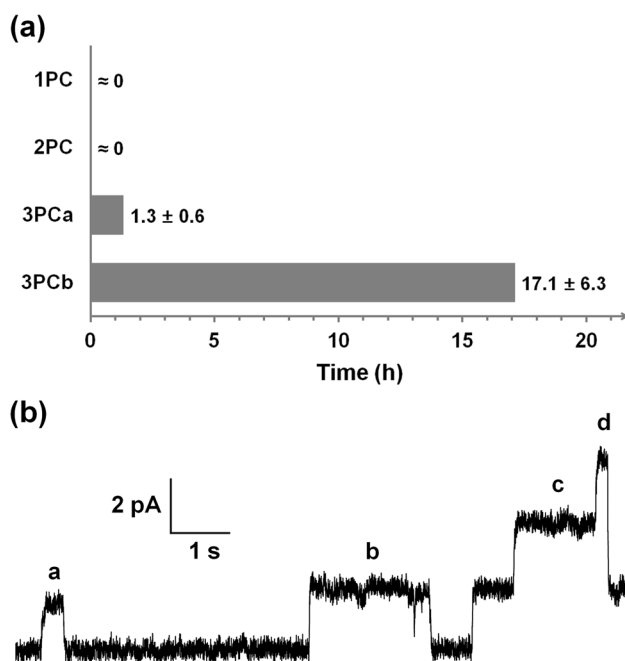


FIG. 5. Electrochemical characterizations of the MSPC-supported BLMs. (a) A comparison of BLM stability with different supporting MSPC membranes. The Arabic numerals prefixed to “PC” denote the number of stacking layers. 1PC and 2PC represent 1-layer and 2-layer PC with the component PC membranes of the same or different pore diameters. 3PCa and 3PCb represent the 3-layer MSPC membranes with pore diameters of $5\ \mu\text{m}|2\ \mu\text{m}|1\ \mu\text{m}$ and $5\ \mu\text{m}|2\ \mu\text{m}|0.4\ \mu\text{m}$, respectively. Five independent measurements are carried out. (b) Channel recording of gramicidin with the applied voltage of 100 mV and the sampling rate of 1 kHz. Both single ((a) and (b)) and multiple ((c) and (d)) channel openings are observed.

To confirm the formation of single BLMs on the MSPC membrane, ion channel recording has been conducted after incorporating ion channels into the lipid bilayers. In this work, gramicidin has been employed to form trans-BLM ion channels because its structure and channel activity are well characterized. When gramicidin solution is injected onto the BLM-formed MSPC membrane ($\sim 25\ \text{nl}$ of $1\ \text{ng ml}^{-1}$ ethanol solution), two gramicidin monomers form one head-to-head dimer in BLM, which serves as the channel for the transmembrane mass transfer of monovalent cations (close-up view in Fig. 4(a)). Fig. 5(b) shows a part of the transmembrane current trace (peak to peak baseline noise of about 0.5 pA) arising from the stochastic opening and closing of the gramicidin channels. The first current level in this steplike signal (a and b in Fig. 5(b)) is about 2 pA corresponding to 20 pS conductance, which is in accordance with the previous results from the study of single gramicidin channels (20–25 pS).^{37,38} The channel lifetimes for a and b events are 0.5 s and 2.1 s, respectively, which are also within the range of lifetimes reported previously.³⁹ These results convince us that the events a and b are the openings of single channels. The second and third current levels are 2 and 3 times higher than the first, respectively, which indicates multiple openings (double for c and triple for d, Fig. 5(b)) also take place quite often.

In order to estimate how many through pores exist in an MSPC membrane and what the fraction of BLM-covered through pores is, we have first measured the capacitance of the BLM-covered membrane. A triangular wave of unit dV/dt slope (Fig. 6(a)) is applied across the membrane. In this condition, the capacitance directly corresponds to the capacitive current (I_C in Fig. 6(b)) because $I_C = C \times dV/dt$. The resulting current signal should show a square wave with the same period of the applied triangular wave. However, our result is very noisy. But, the top-to-bottom average value could be measured to be about 2.8 pA. Therefore, the capacitance of our BLM-covered MSPC membrane is about 1.4 pF. The corresponding lipid bilayer area is calculated to be about $22\ \mu\text{m}^2$, on the basis of the reported specific capacitance of $6.5\ \mu\text{F cm}^{-2}$ for DPhPC bilayers over submicropores.^{8,40} As pores of PC membranes are randomly distributed,⁴¹ the density of through pores cannot be directly estimated from the cross-sections observed by

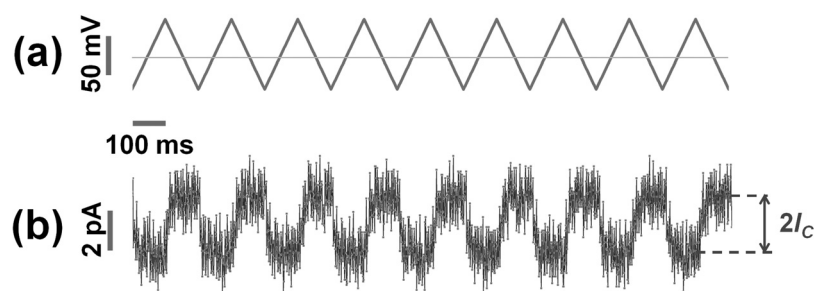


FIG. 6. (a) The triangular voltage wave applied to the BLM-covered MSPC membrane: 50 mV amplitude and 5 Hz frequency. (b) The resulting current signal. $2I_C$ is the average of top-to-bottom values.

microscopy (Figs. 4(b) and 4(c)). Based on pore densities of the component PC membranes, the pores of the bottom-most PC membrane are blocked by a factor of 200, giving the total through pore area to be about $150 \mu\text{m}^2$. It can be, therefore, estimated that about 15% of through pores are covered by lipid bilayers (see supplementary material²⁰ for the details). Since there is a high possibility for the pores of the bottom-most membrane to be partially covered by the upper component membrane, generating the non-circular through pores with smaller pore sizes, those pores are more likely to be filled with lipid solution, rather than being spanned with lipid bilayers, which contribute the major portion (85%) of through pores.

IV. CONCLUSION

In conclusion, the formation of pore-spanning, single BLMs in a PDMS-based microfluidic system has been achieved through our developments of the economical fabrication technique of submicropores from commercially available PC membranes, the epoxy-based bonding technique, and the versatile on-site injection method. The stacking approach blocks the pores of the bottom-most layer by a factor of about 200. As the pore diameter is in the sub-microscale, the reconstitution of functional ion channels (like gramicidin, alpha-hemolysin, etc.) by self-insertion mode is thus more suitable than the method of proteoliposome fusion. At the present stage, the accessibility to the on-site injection technique may be somewhat restricted due to the use of micromanipulators. If such restriction can be relieved by some technical ways in the future, this nano-injection strategy could play a role in extending the present system to multistation ones with different kinds of ion channels. In such multistation/array devices, each station would be equipped with an independent on-site injector and also an embedded Ag/AgCl electrode, which would enable highly parallelized ion channel recording. This kind of systems could revolutionize ion channel drug screening that demands high throughput but low cost.

ACKNOWLEDGMENTS

J. H. Hahn gratefully acknowledges the financial support from the Basic Science Research Program (NRF-2010-0024306) of the National Research Foundation, Ministry of Education, Science and Technology, South Korea. C. Ban thanks the National Research Foundation of Korea for their financial support for this work (NRF-2014029297).

¹B. Alberts, A. Johnson, J. Lewis, M. Raff, K. Roberts, and P. Walter, *Molecular Biology of the Cell*, 5th ed. (Garland Science, New York, 2007).

²Q. Y. He and J. F. Chiu, *J. Cell. Biochem.* **89**(5), 868 (2003).

³E. Neher and B. Sakmann, *Nature* **260**(5554), 799 (1976).

⁴P. Mueller, D. O. Rudin, H. Ti Tien, and W. C. Wescott, *Nature* **194**(4832), 979 (1962).

⁵S. Kalsi, A. M. Powl, B. A. Wallace, H. Morgan, and M. R. de Planque, *Biophys. J.* **106**(8), 1650 (2014).

⁶A. Oshima, A. Hirano-Iwata, H. Mozumi, Y. Ishinari, Y. Kimura, and M. Niwano, *Anal. Chem.* **85**(9), 4363 (2013).

⁷W. Römer and C. Steinem, *Biophys. J.* **86**(2), 955 (2004).

⁸X. J. Han, A. Studer, H. Sehr, I. Geissbuhler, M. Di Berardino, F. K. Winkler, and L. X. Tiefenauer, *Adv. Mater.* **19**(24), 4466 (2007).

⁹R. J. White, E. N. Ervin, T. Yang, X. Chen, S. Daniel, P. S. Cremer, and H. S. White, *J. Am. Chem. Soc.* **129**(38), 11766 (2007).

- ¹⁰S. Steltenkamp, M. M. Müller, M. Deserno, C. Hennesthal, C. Steinem, and A. Janshoff, *Biophys. J.* **91**(1), 217 (2006).
- ¹¹S. Y. Teh, R. Khnouf, H. Fan, and A. P. Lee, *Biomicrofluidics* **5**(4), 044113 (2011).
- ¹²M. Takinoue and S. Takeuchi, *Anal. Bioanal. Chem.* **400**(6), 1705 (2011).
- ¹³M. Zagnoni, *Lab Chip* **12**(6), 1026 (2012).
- ¹⁴M. A. Czekalska, T. S. Kaminski, S. Jakiela, K. Tanuj Sapra, H. Bayley, and P. Garstecki, *Lab Chip* **15**(2), 541 (2015).
- ¹⁵J. Shim, J. Geng, C. Ahn, and P. Guo, *Biomed. Microdev.* **14**(5), 921 (2012).
- ¹⁶V. C. Stimberg, J. G. Bomer, I. van Uitert, A. van den Berg, and S. Le Gac, *Small* **9**(7), 1076 (2013).
- ¹⁷W. Wang, L. Monlezun, M. Picard, P. Benas, O. Francais, I. Broutin, and B. Le Pioufle, *Analyst* **137**(4), 847 (2012).
- ¹⁸R. Kawano, T. Osaki, H. Sasaki, and S. Takeuchi, *Small* **6**(19), 2100 (2010).
- ¹⁹M. Zagnoni, M. E. Sandison, P. Marius, A. G. Lee, and H. Morgan, *Lab Chip* **7**(9), 1176 (2007).
- ²⁰See supplementary material at <http://dx.doi.org/10.1063/1.4919066> for expanded materials and methods section, supplementary figures and tables, SI–SV measurement for the BLM-free and BLM-covered MSPC, determination of bilayer capacitance, and total through pore area of MSPC membrane.
- ²¹R. H. Estes, EPO-TEK[®] Technical Paper No. 38, “The suitability of epoxy-based adhesives for use in medical devices An overview of adhesives in medical applications,” available at <http://www.epotek.com/site/technical-material/technical-material.html>.
- ²²B. H. Chueh, D. Huh, C. R. Kyrtos, T. Houssin, N. Futai, and S. Takayama, *Anal. Chem.* **79**(9), 3504 (2007).
- ²³K. Aran, L. A. Sasso, N. Kamdar, and J. D. Zahn, *Lab Chip* **10**(5), 548 (2010).
- ²⁴Model P-2000 micropipet puller—operation manual V.2.2 (Sutter Instrument Co., USA, 2010).
- ²⁵Model BV-10 micropipette beveler—operation manual V.2.10 (Sutter Instrument Co., USA, 2010).
- ²⁶J. N. Lee, C. Park, and G. M. Whitesides, *Anal. Chem.* **75**(23), 6544 (2003).
- ²⁷N. Malmstadt, M. A. Nash, R. F. Purnell, and J. J. Schmidt, *Nano Lett.* **6**(9), 1961 (2006).
- ²⁸L. C. M. Gross, A. J. Heron, S. C. Baca, and M. I. Wallace, *Langmuir* **27**(23), 14335 (2011).
- ²⁹B. Liu, D. Rieck, B. J. Van Wie, G. J. Cheng, D. F. Moffett, and D. A. Kidwell, *Biosens. Bioelectron.* **24**(7), 1843 (2009).
- ³⁰L. J. Heyderman, B. Ketterer, D. Bächle, F. Glaus, B. Haas, H. Schiff, K. Vogelsang, J. Gobrecht, L. Tiefenauer, O. Dubochet, P. Surbled, and T. Hessler, *Microelectron. Eng.* **67–68**(0), 208 (2003).
- ³¹M. A. Dhoke, P. J. Ladha, F. J. Boerio, L. B. Lessard, D. H. Malinowska, J. Cuppoletti, and D. S. Wiczorek, *Biochim. Biophys. Acta* **1716**(2), 117 (2005).
- ³²R. Hemmler, G. Böse, R. Wagner, and R. Peters, *Biophys. J.* **88**(6), 4000 (2005).
- ³³G. Favero, A. D’Annibale, L. Campanella, R. Santucci, and T. Ferri, *Anal. Chim. Acta* **460**(1), 23 (2002).
- ³⁴T. Navrátil, I. Šestáková, K. Štulík, and V. Mareček, *Electroanalysis* **22**(17–18), 2043 (2010).
- ³⁵T. Phung, Y. Zhang, J. Dunlop, and J. E. Dalziel, *Int. J. Electrochem.* **2011**, 213107.
- ³⁶W. Römer, Y. H. Lam, D. Fischer, A. Watts, W. B. Fischer, P. Göring, R. B. Wehrspohn, U. Gösele, and C. Steinem, *J. Am. Chem. Soc.* **126**(49), 16267 (2004).
- ³⁷V. S. Rudnev, L. N. Ermishkin, L. A. Fonina, and Y. G. Rovin, *BBA–Biomembr.* **642**(1), 196 (1981).
- ³⁸S. Futaki, Y. Zhang, T. Kiwada, I. Nakase, T. Yagami, S. Oiki, and Y. Sugiura, *Bioorg. Med. Chem.* **12**(6), 1343 (2004).
- ³⁹S. B. Hladky and D. A. Haydon, *BBA–Biomembr.* **274**(2), 294 (1972).
- ⁴⁰Z. W. Zhu, Y. Wang, X. Zhang, C. F. Sun, M. G. Li, J. W. Yan, and B. W. Mao, *Langmuir* **28**(41), 14739 (2012).
- ⁴¹M. Cheryan and M. Cheryan, *Ultrafiltration and Microfiltration Handbook* (Technomic Pub. Co., Lancaster, PA, 1998).